Vol 10 No 9, September 2001
1009-1963/2001/10(09)/0783-04

Chinese Physics

© 2001 Chin. Phys. Soc.
and IOP Publishing Ltd

OPTICAL SPACE OF THE KERR SOLUTIONS*

Lü Jun-li(吕君丽)

Department of Physics, Hunan Normal University, Changsha 410081, *China*

(Received 6 November 2000; revised manuscript received 5 May 2001)

In this paper, we discuss the optical geometry of the Kerr solutions, and show the embedding diagram at the equator $\theta = \pi/2$ for the optical space of the Kerr solution with $a/M = 1$. It is noticed that at the equator $\theta = \pi/2$, the Gaussian curvature K for the ordinary space is negative, and the $\widetilde{K}$ for the optical space is positive.

Keywords: optical geometry, embedding diagrams, Gaussian curvatures
PACC: 0420

I. INTRODUCTION

In the study of the properties of a spacetime described by a metric $g_{\mu\nu}$, it is often useful to examine the geometry of a hypersurface in it with embedding diagrams. Furthermore, an optical space construction often proves useful. We choose a metric $\tilde{g}_{ij}$ on the hypersurface which is not simply the induced metric γ_{ij} (projection of $g_{\mu\nu}$ onto the hypersurface) but rather a metric conformally related to it, $\tilde{g}_{ij} = \sigma^{-2}\gamma_{ij}$.[1−3] Abramowicz *et al.*[2] suggested the choice of $\sigma^2 = -g_{tt}$. The resulting Riemannian metric $\tilde{g}_{ij}$ is referred to as the "optical geometry". In a stationary or static background spacetime, interesting properties of particle dynamics are described by the optical geometry. For example, in the static case the geodesics of the optical space are "optically straight ", in the sense that they coincide with the trajectories of light rays.[2−6]

Embedding diagrams have been used extensively to study the properties of hypersurfaces in curved spacetimes. In the method of embedding diagrams, a hypersurface in a higher dimensional spacetime is represented by a curved surface in a fiducial flat space having the same intrinsic curvature as the hypersurface being studied. However, embedding diagrams of the optical space have been presented in the literature only for the Schwarzschild solution and for the Reissner–Nordström solution.[2,4] In this paper, we extend the effort to the study of the optical geometry of the Kerr solutions.

II.THE OPTICAL GEOMETRY FOR KERR SOLUTIONS

The Kerr solution in Boyer and Lindquist coordinates (t, r, θ, ϕ) can be written as[7]

$$\begin{aligned} \mathrm{d}s^2 = &-\left(1-\frac{2Mr}{\rho^2}\right)\mathrm{d}t^2 \\ &+\frac{\rho^2}{\Delta}\mathrm{d}r^2+\rho^2\mathrm{d}\theta^2+\left[(r^2+a^2)\right. \\ &\left.+\frac{2a^2Mr\sin^2\theta}{\rho^2}\right]\sin^2\theta\mathrm{d}\phi^2 \\ &-\frac{4aMr\sin^2\theta}{\rho^2}\mathrm{d}t\mathrm{d}\phi, \end{aligned} \tag{1}$$

where $\rho^2 = r^2 + a^2\cos^2\theta$ and $\Delta = r^2 - 2Mr + a^2$. M and a are constants, M representing the mass and Ma the angular momentum as measured from infinity. When $a = 0$, the solution reduces to the Schwarzschild solution.

The three-dimensional (3D) space metric γ_{ij} can be read out from the full four-dimensional metric by decomposing it in the form

$$\mathrm{d}s^2 = \mathrm{d}l^2 - \Phi(\mathrm{d}t + 2\alpha_i\mathrm{d}x^i)^2, \tag{2}$$

$$\mathrm{d}l^2 = \gamma_{ij}\mathrm{d}x^i\mathrm{d}x^j, \tag{3}$$

which is equivalent to setting

$$g_{00} = -\Phi, \quad g_{0i} = -2\Phi\alpha_i, \quad g_{ij} = \gamma_{ij} - 4\Phi\alpha_i\alpha_j, \tag{4}$$

where $\Phi = (1 - 2Mr/\rho^2)$ and $\alpha_\phi = aMr\sin^2\theta/(\rho^2 - 2Mr)$ for the Kerr solution. So the positive-defined metric induced from Eq.(1) has the form

$$\begin{aligned} \mathrm{d}l^2 =&\gamma_{ij}\mathrm{d}x^i\mathrm{d}x^j \\ =&\frac{\rho^2}{\Delta}\mathrm{d}r^2+\rho^2\mathrm{d}\theta^2+\frac{\Delta}{1-\dfrac{2Mr}{\rho^2}}\sin^2\theta\mathrm{d}\phi^2. \end{aligned} \tag{5}$$

*Project supported by the National Natural Science Foundation of China (Grant No. 19874020).

Let us introduce the optical metric $\tilde{g}_{ij} = \Phi^{-1}\gamma_{ij}$, and obtain the line element of the optical space for the Kerr solution

$$\begin{aligned} \mathrm{d}\tilde{l}^2 =& \tilde{g}_{ij}\mathrm{d}x^i\mathrm{d}x^j \\ =& \frac{\rho^2}{\left(1-\frac{2Mr}{\rho^2}\right)\Delta}\mathrm{d}r^2 + \frac{\rho^2}{\left(1-\frac{2Mr}{\rho^2}\right)}\mathrm{d}\theta^2 \\ &+ \frac{\Delta}{\left(1-\frac{2Mr}{\rho^2}\right)^2}\sin^2\theta\mathrm{d}\phi^2. \end{aligned} \tag{6}$$

In accordance with the definition, Eq.(2) is rewritten as

$$\mathrm{d}s^2 = \Phi[\mathrm{d}\tilde{l}^2 - (\mathrm{d}t + 2\alpha_i\mathrm{d}x^i)^2]. \tag{7}$$

Next, we discuss some geometrical features near the external horizon $r = r_{\mathrm{H}} = M + \sqrt{M^2 - a^2}$.

We examine the proper lengths x and $\tilde{x}$ along radial directions according to the metrics (5) and (6), and obtain

$$\mathrm{d}x = \sqrt{\frac{\rho^2}{\Delta}}\mathrm{d}r, \tag{8}$$

$$\mathrm{d}\tilde{x} = \sqrt{\frac{\rho^2}{\Phi\Delta}}\mathrm{d}r. \tag{9}$$

We have asymptotically, for the Kerr metric in the region $r \approx r_{\mathrm{H}}$,

$$x \approx \begin{cases} \dfrac{\sqrt{2(r_{\mathrm{H}}^2 + a^2\cos^2\theta)}}{(M^2-a^2)^{1/4}}\sqrt{r - r_{\mathrm{H}}} & \text{for } a < M, \\ M\sqrt{1+\cos^2\theta}\ln\left(\dfrac{r}{M} - 1\right) & \text{for } a = M, \end{cases} \tag{10}$$

and

$$\tilde{x} \approx \begin{cases} \dfrac{(r_{\mathrm{H}}^2 + a^2\cos^2\theta)}{2\sqrt{M^2-a^2}}\ \mathrm{Arth}\sqrt{\dfrac{2(r-r_{\mathrm{H}}) - a^2\sin^2\theta/\sqrt{M^2-a^2}}{2(r-r_{\mathrm{H}})}} & \text{for } a < M, \\ \dfrac{M(1+\cos^2\theta)}{\sin\theta}\mathrm{arc\ sec}\left(\dfrac{r-M}{M\sin\theta}\right) & \text{for } a = M. \end{cases} \tag{11}$$

From Eqs.(10) and (11), we notice that: (i) the proper lengths x and $\tilde{x}$ along the radial direction are dependent on θ, and for $a < M$, at the equator are smaller than in the poles; (ii) for $a < M$, in the poles ($\theta = 0, \pi$) the horizon is located at a finite proper distance in the ordinary space, but is infinitely far away according to the optical geometry.

At the event horizon $r = r_{\mathrm{H}} = M + \sqrt{M^2 - a^2}$, the Gaussian curvatures K and $\tilde{K}$ of the two-surface described by the metrics (5) and (6) are given, respectively, by[8,9]

$$K = -\frac{\left[\gamma'_{33}/\sqrt{\gamma_{22}\gamma_{33}}\right]'}{2\sqrt{\gamma_{22}\gamma_{33}}}, \tag{12}$$

and

$$\tilde{K} = -\frac{\left[\tilde{g}'_{33}/\sqrt{\tilde{g}_{22}\tilde{g}_{33}}\right]'}{2\sqrt{\tilde{g}_{22}\tilde{g}_{33}}}, \tag{13}$$

where the prime denotes differentiation with respect to the polar angle θ. The calculated K and $\tilde{K}$ have quite complex expressions. We discuss some cases of particular interest instead of giving the full expressions. (i) For the extreme Kerr black hole ($a = M$), the curvatures of the event horizon ($r_{\mathrm{H}} = M$) are

$$K = \frac{(2 - 3\sin^2\theta)}{M^2(1+\cos^2\theta)^3}, \tag{14}$$

and

$$\tilde{K} = \frac{(7\sin^4\theta - 8\sin^2\theta + 4)}{M^2(1+\cos^2\theta)^4}. \tag{15}$$

One sees that the curvatures of the event horizon are dependent on θ. When $\theta = 0$, $K = \tilde{K} = \dfrac{1}{4M^2}$. When $\theta = \pi/2$, $K = -\dfrac{1}{M^2}$, and $\tilde{K} = \dfrac{3}{M^2}$. Analysing Eqs.(14) and (15) , we obtain that the curvature of the two-surface for the ordinary space becomes negative for $54.7^\circ \le \theta \le \pi - 54.7^\circ$, and the curvatures of the two-surface for the optical space is always positive. (ii) At the equator $\theta = \pi/2$, the curvatures are

$$K = \frac{r^2(r-2M) + 2Ma^2}{r^4(r-2M)}, \tag{16}$$

and

$$\tilde{K} = \frac{r^2(r-2M) + 4Ma^2}{r^5}. \tag{17}$$

At the horizon r_{H}, the curvatures reduce to

$$K = -\frac{a^2}{(M + \sqrt{M^2-a^2})^4}, \tag{18}$$

and

$$\tilde{K} = \frac{a^2(3M - \sqrt{M^2-a^2})}{(M+\sqrt{M^2-a^2})^5}. \tag{19}$$

One notices that, at the horizon, the curvature K for the ordinary space is always negative, and the curvature $\tilde{K}$ for the optical space is always positive. Qualitative analysis shows that the larger the angular momentum of the black hole, the more curved is the equator surface. For the extreme Kerr black hole ($a = M$), $K = -\frac{1}{M^2}$ and $\tilde{K} = \frac{3}{M^2}$. For $a = 0$ (Schwarzschild solution), $K = 0$ and $\tilde{K} = 0$.

III. EMBEDDING DIAGRAMS

For visualization of the intrinsic geometry of the optical space, we attempt to embed Eqs.(5) and (6) in the Euclidean space. Of course, this is not always possible. We consider only the embedding diagrams of the section corresponding to $\theta = \pi/2$. In the Euclidean 3D space with a metric

$$\mathrm{d}s^2 = \mathrm{d}\overline{r}^2 + \overline{r}^2\mathrm{d}\overline{\phi}^2 + \mathrm{d}z^2, \tag{20}$$

we find a surface $z = z(\overline{r})$ which is isometric to the section $\theta = \pi/2$. This is easily accomplished by writing the metric on the surface as[10]

$$\mathrm{d}s^2 = \left[1 + \left(\frac{\mathrm{d}z}{\mathrm{d}\overline{r}}\right)^2\right]\mathrm{d}\overline{r}^2 + \overline{r}^2\mathrm{d}\overline{\phi}^2, \tag{21}$$

and then identifying it with either $\mathrm{d}l^2$ or $\mathrm{d}\tilde{l}^2$.

Comparing Eq.(21) with Eq.(5), one finds $\overline{\phi} = \phi$,

$$\left(\frac{\mathrm{d}z}{\mathrm{d}\overline{r}}\right)^2 = \frac{r^2}{\Delta(\mathrm{d}\overline{r}/\mathrm{d}r)^2} - 1, \tag{22}$$

and

$$\overline{r}^2 = \frac{\Delta}{1 - \dfrac{2M}{r}}. \tag{23}$$

It is evident from Eq.(22) that to embed Eq.(5) in the Euclidean 3D space, the following condition must be satisfied:

$$2r(r - 2M)^2\Delta - Ma^4 \geq 0. \tag{24}$$

The embedding condition does indeed restrict the portion of the space that can be embedded in the Euclidean 3D space. When $a = 0$ (Schwarzschild solution), the embedding condition (24) reduces to $r \geq r_0 = r_{\mathrm{H}} = 2M$. For the extreme Kerr black hole ($a = M$), Eq.(24) becomes $r \geq r_0 \approx 2.35M$. The behaviour of r_0/M as a function of a/M is shown in Fig.1 (dashed curve). From Eq.(22), we can write straightforwardly

$$z(\overline{r}) = \pm \int_{r_0}^{r(\overline{r})} \frac{1}{\sqrt{r - 2M}} \cdot \sqrt{2M - \frac{M^2a^4}{r(r - 2M)^2\Delta}}\mathrm{d}r + \mathrm{const.}, \tag{25}$$

which, together with Eq.(23), specifies completely the dependence of z on $\overline{r}$.

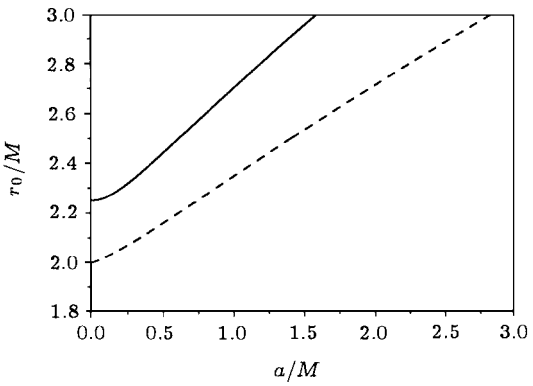


Fig.1. The behaviour of $\tilde{r}_0/M$ (solid curve), and r_0/M (dashed curve) as functions of a/M. r_0 and $\tilde{r}_0$ are the limit of embeddability for the ordinary space and the optical space, respectively.

Now, we turn our attention to the more dynamically informative optical metric (6). Comparing Eq.(21) with Eq.(6), we have

$$\left(\frac{\mathrm{d}z}{\mathrm{d}\overline{r}}\right)^2 = \frac{r^2}{\left(1 - \dfrac{2M}{r}\right)\left(\dfrac{\mathrm{d}\overline{r}}{\mathrm{d}r}\right)^2\Delta} - 1, \tag{26}$$

and

$$\overline{r}^2 = \frac{\Delta}{\left(1 - \dfrac{2M}{r}\right)^2}. \tag{27}$$

Integrating Eq.(26) gives

$$z(\overline{r}) = \pm \int_{\tilde{r}_0}^{r(\overline{r})} \frac{1}{\left(1 - \dfrac{2M}{r}\right)\sqrt{\Delta}} \sqrt{r^2\left(1 - \frac{2M}{r}\right) - \left[(r - 3M) - \frac{2Ma^2}{r^2\left(1 - \dfrac{2M}{r}\right)}\right]^2}\,\mathrm{d}r + \mathrm{const.}, \tag{28}$$

with the embedding condition

$$r^2\left(1 - \frac{2M}{r}\right) - \left[(r - 3M) - \frac{2Ma^2}{r^2\left(1 - \dfrac{2M}{r}\right)}\right]^2 \geq 0. \tag{29}$$

When $a = 0$, the embedding condition reduces to $r \geq \tilde{r}_0 = \frac{9}{4}M$. For the extreme Kerr black hole ($a = M$), the embedding condition becomes $r \geq \tilde{r}_0 \approx 2.7M$. Figure 1 (solid curve) shows the behaviour of $\tilde{r}_0/M$. It is evident that the embedded space for the optical space is restricted, as compared with the ordinary space (see Fig.1).

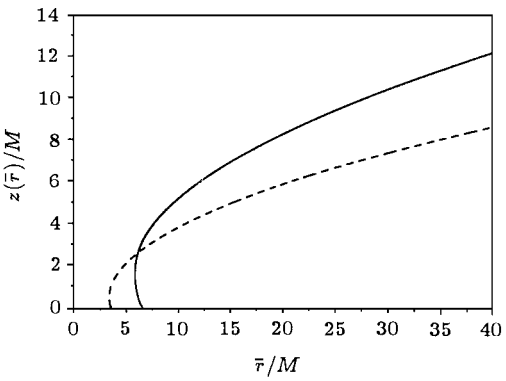


Fig.2. The function $z(\overline{r})$ for the ordinary space (dashed curve) and the optical space (solid curve) of the Kerr solution with $a/M = 1$.

For comparison, the behaviours of $z(\overline{r})/M$ with respect to $\overline{r}/M$ for the ordinary space and the optical space of the Kerr solution with $a/M = 1$ are shown on the same diagram in Fig.2. The embedding diagram for the optical space at $\theta = \pi/2$ is shown in Fig.3. It is noted that this embedding of the optical metric (6) for the section $\theta = \pi/2$ shares with the ordinary metric (5) the property that $\mathrm{d}z/\mathrm{d}\overline{r}$ tends to zero at infinity, with the conformal factor going to one asymptotically. The equatorial sections for both the ordinary space and the optical space cannot be globally embedded in 3D Euclidean flat space all the way into the horizon at $r_{\mathrm{H}} = M + \sqrt{M^2 - a^2}$. From Eqs.(16) and (17), examining their curvatures in the limit of embeddability (i.e. at $r_0 \approx 2.35M$, and $\tilde{r}_0 \approx 2.7M$) gives $K \approx 0.368/M^2$ and $\tilde{K} \approx 0.063/M^2$.

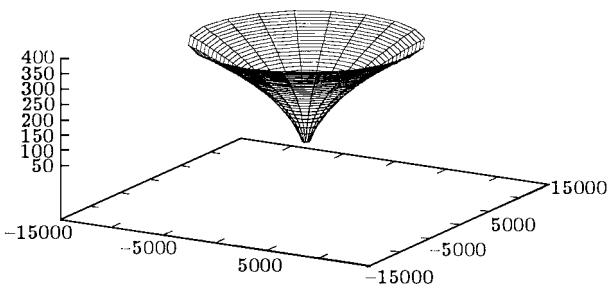


Fig.3. The embedding diagram for the optical space of the Kerr solution with $a = M$ at the equator $\theta = \pi/2$.

References

[1] Dowker J S and Kennedy G 1978 *J. Phys. A: Math. Gen.* **11** 895

[2] Abramowicz M A, Carter B and Lasota J P 1988 *Gen. Relativ. Gravit.* **20** 1173

[3] Kristiansson S, Sonego S and Abramowicz M A 1998 *Gen. Relativ. Gravit.* **30** 275

[4] Gibbons G W and Perry M J 1978 *Proc. R. Soc.* A **358** 467

[5] Kuang Z Q and Liang C B 1994 *Acta Phys. Sin. (Overseas Edition)* **3** 881

[6] Kuang Z Q and Liang C B 1996 *Acta Phys. Sin. (Overseas Edition)* **5** 641

[7] Chandrasekhar S 1983 *The Mathematical Theory of Black Holes* (Oxford: Oxford University Press) p 289

[8] Weinberg S 1980 *Gravitation and Cosmology* (Beijing: Science Press) p 83 (in Chinese)

[9] Kokkotas K D 1988 *Gen. Relativ. Gravit.* **20** 829

[10] Misner C W, Thorne K S and Wheeler J A 1973 *Gravitation* (San Francisco: Freeman) p 613